Supporting Information for

Computational insights on potential dependence of electrocatalytic synthesis of ammonia from nitrate

Huijuan Jing [a,b], Jun Long [a], Huan Li [a,b], Xiaoyan Fu [a], Jianping Xiao [a,b,*]

[a] *State Key Laboratory of Catalysis, Dalian National Laboratory for Clean Energy, Dalian Institute of Chemical Physics, Chinese Academy of Sciences,*
Dalian 116023, Liaoning, China
[b] *University of Chinese Academy of Sciences, Beijing 100049, China*

[*] Corresponding author. E-mail: xiao@dicp.ac.cn (J.Xiao).

Computational details

Adsorption and reaction free energies. We calculated all the adsorption energies and structures of intermediates for ammonia and nitrite production on six MN_4 (M = Fe, Co, Ni, Cu, V, Sc) single atom catalysts, as shown in **Table S2** and **S3**. The solvation effect was considered to correct the adsorption free energies. We used the implicit solvation model implemented in VASPsol[1] to explicitly calculate solvation energy (E_{sol}), with the water dielectric constant of 78.5. **Table S5** lists all the E_{sol} over FeN_4 used in this work. The adsorption energy (E_{ad}) was defined as

$$E_{ad} = E_{tot} - E_{slab} - (xE_H + yE_N + zE_O) \qquad \text{eq S1}$$

where E_{tot} and E_{slab} are the total energies of the surfaces with adsorbates and the bare ones, respectively. $E_H = 1/2\ E_{H_2}$, $E_O = E_{H_2O} - E_{H_2}$, $E_N = 1/2\ E_{N_2}$. x, y, z represents the number of hydrogen, oxygen, nitrogen atoms in intermediates. The adsorption free energy (G_{ad}) and reaction energies (ΔE) were calculated with the following eq S2 and S3:

$$G_{ad} = E_{ad} + \Delta E_{ZPE} - T\Delta S + \Delta E_{sol} \qquad \text{eq S2}$$

$$\Delta E = E_P - E_R \qquad \text{eq S3}$$

While the reaction free energies (ΔG) were calculated using computational hydrogen electrode (CHE) model[2] under 298.15 K with the following equation:

$$\Delta G = \Delta E + \Delta E_{ZPE} - T\Delta S + \Delta E_{sol} + e(U - U_0) \qquad \text{eq S4}$$

where ΔE_{ZPE}, T, ΔS represent the difference of zero-point vibrational energy between the products and reactants, thermodynamic temperature, entropy change, respectively. ΔE_{sol} is the solvation energy, e is the energy of the electron, U and U_0 refer to the applied electrode potential and 0V versus RHE, respectively. The $\Delta E_{ZPE} - T\Delta S$ of the intermediates involved in reaction are shown in **Table S4**. The zero-point energies and entropies of gas phase molecules were obtained from NIST database as listed in **Table S6**.

Potential-dependent protonation barriers. The potential-dependent electrochemical barriers were calculated using the "charge-extrapolation" method, proposed by Chan and Nørskov[3-4]. For an elementary reaction, the transition state (TS) was searched by the climbing image nudged elastic band (CI-NEB) method[5]. A monolayer of water containing a hydronium (H_3O^+) ion, which acts as the proton source, was placed on the catalyst surface to calculate the barrier of proton coupling electron transfer reaction. The conditions of the experimental results are used as the benchmark, although the experimentally neutral pH is considered to be the proton source from H_2O, and H_3O^+ as proton source to transfer can approximately simulate such a process, which has been successfully used in previous studies[6-7]. As there is good linear correlations between the calculated surface charge transfer (q) and potential (U) variation at IS, TS, and FS, so a capacitor model was employed to calculate the barrier at a given potential[8]. For a constant charge CI-NEB calculation, the energy change from state 1 to state 2 (state 1 and state 2 are any two of initial, transition and final states) at constant work functions, Φ_1 and Φ_2 (1 and 2 here are considered IS and TS), can be given by

$$E_2(\Phi_1) - E_1(\Phi_1) = E_2(\Phi_2) - E_1(\Phi_1) + \frac{(q_2 - q_1)(\Phi_2 - \Phi_1)}{2} \qquad \text{eq S5}$$

$$E_2(\Phi_2) - E_1(\Phi_2) = E_2(\Phi_2) - E_1(\Phi_1) - \frac{(q_2 - q_1)(\Phi_2 - \Phi_1)}{2} \qquad \text{eq S6}$$

Setting $\Delta E(\Phi) = E_2(\Phi) - E_1(\Phi)$ at a constant work function Φ and $\Delta q = q_2 - q_1$, it can derive the following equation:

$$\Delta E(\Phi_2) - \Delta E(\Phi_1) = -\Delta q(\Phi_2 - \Phi_1) \qquad \text{eq S7}$$

where $\Delta E(\Phi_2)$ and $\Delta E(\Phi_1)$ are the barriers at given Φ_2 and Φ_1, respectively. Taking Φ_1 as the reference work function, Φ_{ref} (e.g., that corresponding to the standard hydrogen electrode potential[9]), and Φ_2 to be the independent variable, we obtained the barriers as a function of Φ_2

$$\Delta E(\Phi_2) = \Delta E(\Phi_{ref}) - \Delta q(\Phi_2 - \Phi_{ref}) \qquad \text{eq S8}$$

The work functions, Φ, can be related to the absolute potential by $U_{SHE} = \frac{\Phi - \Phi_{SHE}}{e}$ and Φ_{SHE} has been determined experimentally to be ~ 4.4 eV[3]. Therefore, the potential-dependent barrier can be calculated by this method. For surface charge transfer (q), the corresponding charge of electrode slab (with adsorbates), which can be obtained via Bader charge calculation. For work function calculations, a dipole correction was applied in *z*-direction.

The elementary steps of eNO$_3$RR. For electrochemical reduction of nitrate, we have considered two whole reactions, as follows:

$$NO_3^- + 9H^+ + 8e^- \rightarrow NH_3 + 3H_2O \qquad \text{eq S9}$$

$$NO_3^- + 3H^+ + 2e^- \rightarrow HNO_2 + H_2O \qquad \text{eq S10}$$

For the above two total reactions there are some elementary reactions that are considered, listed in Table S1. Note that these elementary reactions other than R0 and R1 are written to proceed via the Heyrovsky route, considering that this route becomes more dominant at high overpotentials[10].

The first elementary step considerations for eNO$_3$RR. There are two forms of consideration for the first elementary step (R0: $NO_3^- + H^+ \rightarrow HNO_3$ and R1: $NO_3^- + H^+ + * \rightarrow HNO_3*$), whose Gibbs reaction free energy[11-12] can be indirectly calculated as follows:

$$NO_3^- + H^+ \rightarrow HNO_3(l) \quad \Delta G_{S11} = 0.317 \text{ eV} \qquad \text{eq S11}$$

$$HNO_3(l) \rightarrow HNO_3(g) \quad \Delta G_{S12} = 0.075 \text{ eV} \qquad \text{eq S12}$$

$$HNO_3(g) + * \rightarrow HNO_3* \quad \Delta G_{S13} = G_{ad}HNO_3* - G_{gas}HNO_3 \qquad \text{eq S13}$$

Therefore, the reaction free energies of elementary R0 and R1 can be respectively approximated as:

$$\Delta G_{R0} = \Delta G_{S11} + \Delta G_{S12} = 0.392 \text{ eV}$$

$$\Delta G_{R1} = \Delta G_{S11} + \Delta G_{S12} + \Delta G_{S13} = G_{ad}HNO_3* - G_{gas}HNO_3 + 0.392$$

Microkinetic simulations. CATKINAS code were used for microkinetic simulations[13-14], based on the potential-dependent barriers and reaction free energies for electrochemical steps. For thermochemical steps, the barriers and reaction free energies were assumed to be constant. For eNO_3RR to NH_3 and to HNO_2, we combine R0 and R2 into an elementary step in the microkinetic simulation, avoiding the problem of HNO_3 partial pressure setting. The reaction rate was calculated following the Arrhenius equation (eq S14) and the surface coverage of adsorbed species was solved with the steady-state approximation (eq S15).

$$r = k\theta_A\theta_B = \frac{k_B T}{h} exp\left(-\frac{G_a}{RT}\right)\theta_A\theta_B \qquad \text{eq S14}$$

$$\frac{\partial \theta_i}{\partial t} = 0 \qquad \text{eq S15}$$

$$\sum_i \theta_i = 1 \qquad \text{eq S16}$$

where r is the reaction rate, k is reaction rate constant, θ_A and θ_B are the surface concentrations of the reactants, k_B is the Boltzmann constant, T is the thermodynamic temperature, G_a is the activation free barrier, and θ_i represents the surface coverage of anyone adsorbed species. The considered elementary steps and kinetic equations have been shown in **Table S10**.

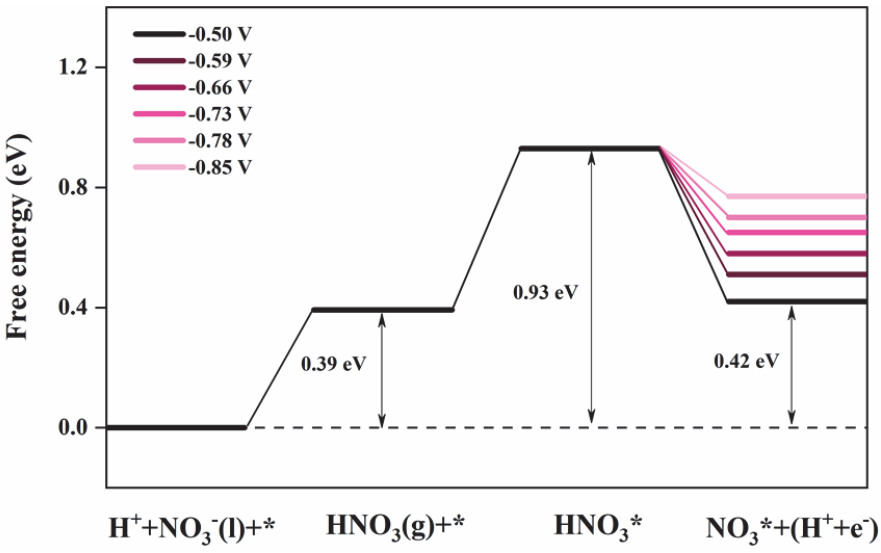

Figure S1. The possible first step reaction free energies on FeN_4 catalyst.

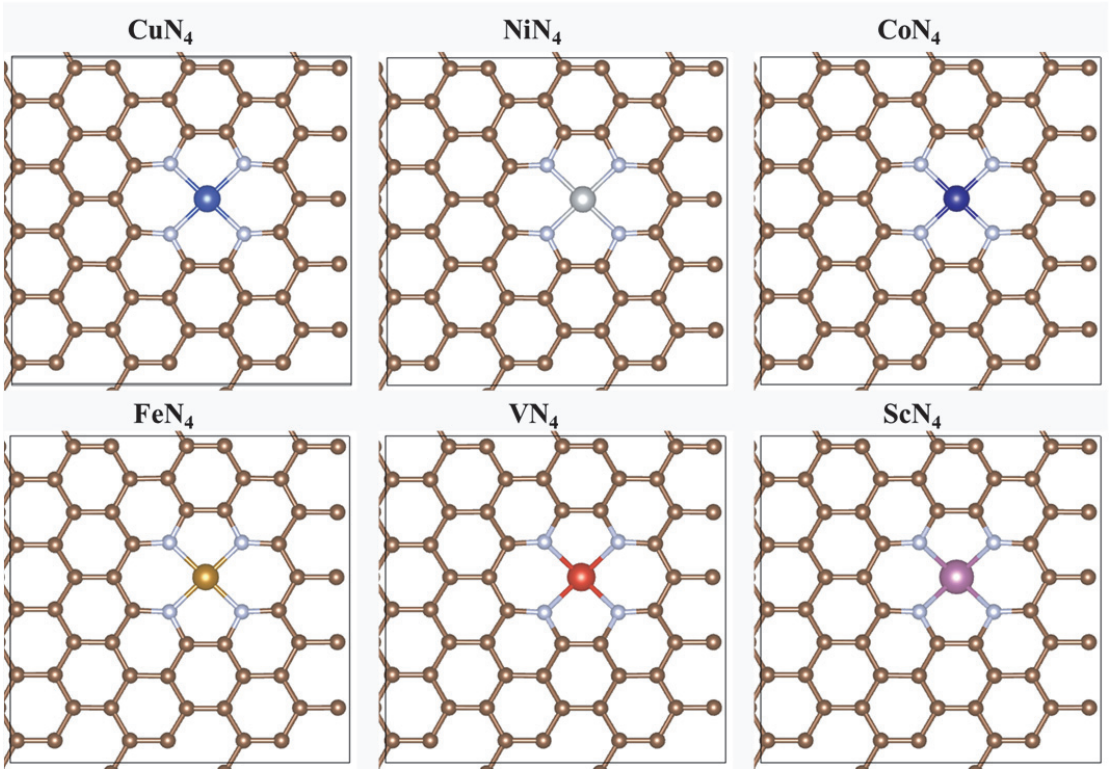

Figure S2. The structures of CuN_4, NiN_4, CoN_4, FeN_4, VN_4 and ScN_4 catalysts.

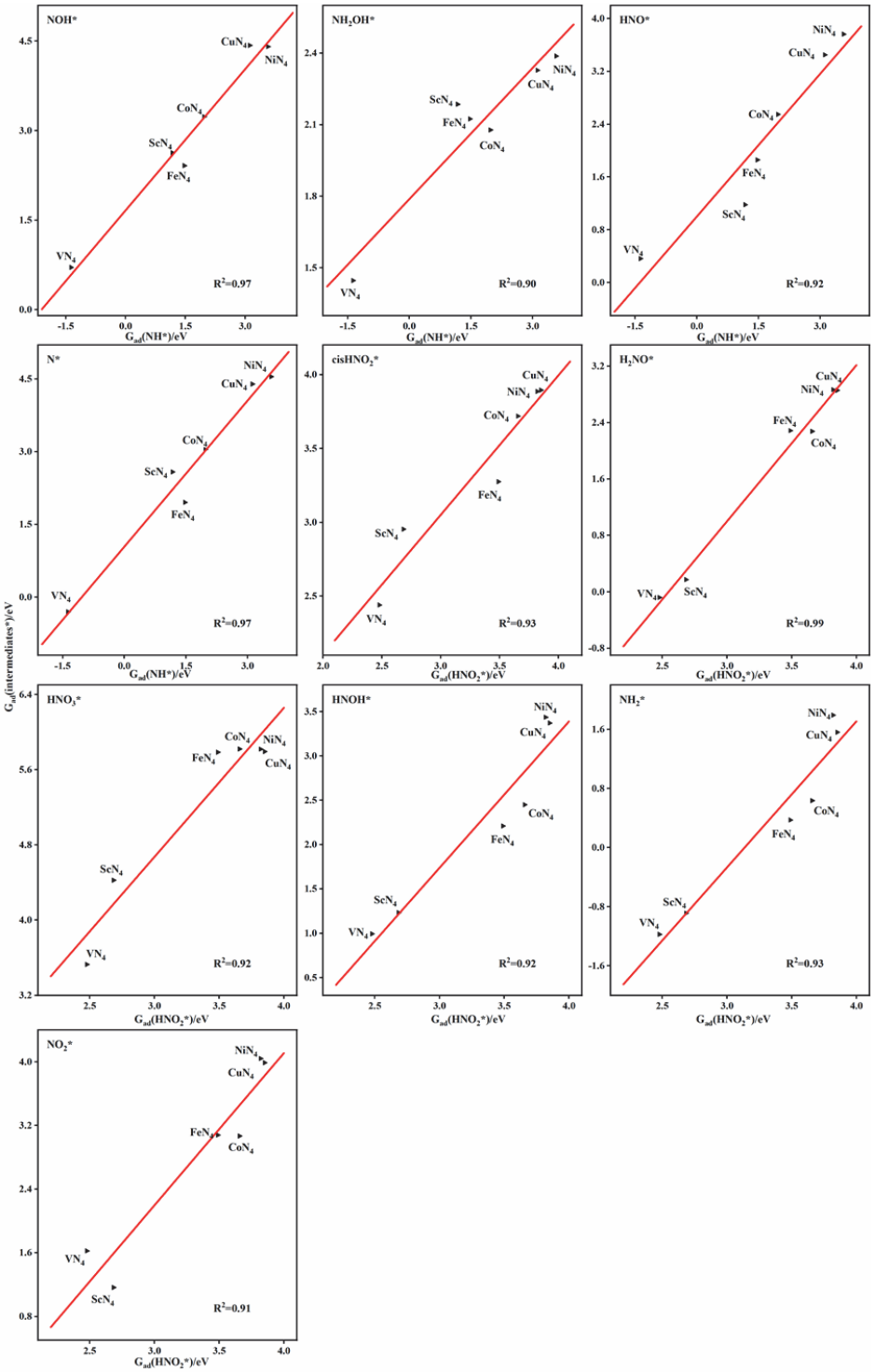

Figure S3. Scaling relations for intermediates involved in eNO_3RR to $NH_3 + HNO_2$, $G_{ad}(NH^*)$ and $G_{ad}(HNO_2^*)$ were chosen as two descriptors.

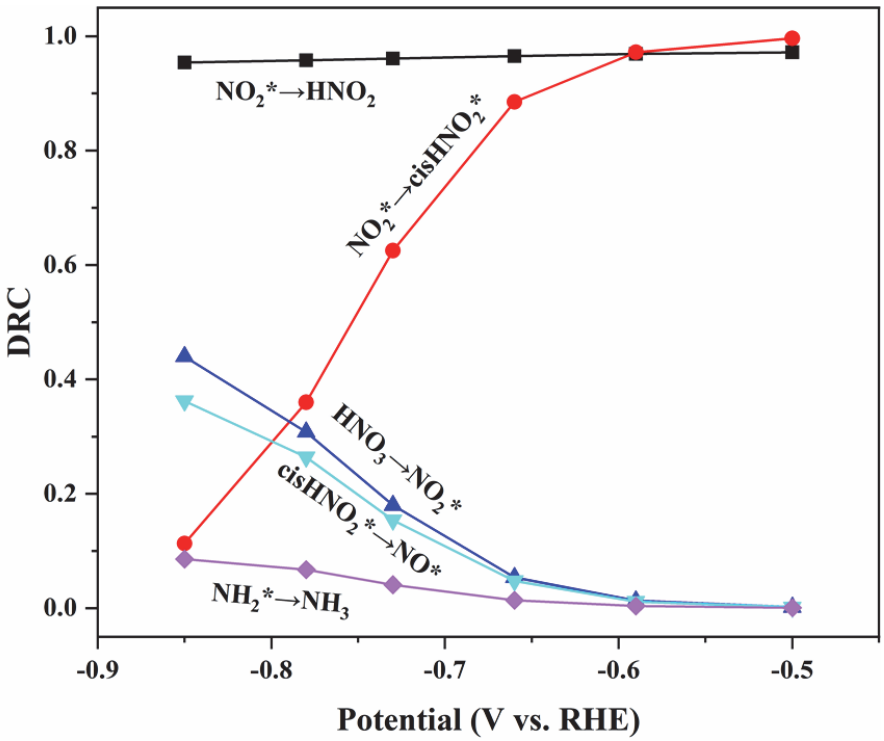

Figure S4. Degree of rate control (DRC) of key elementary steps in eNO_3RR.

Table S1. The 22 elementary steps considered for eNO_3RR process.

Number	Elementary reactions	Number	Elementary reactions
R0	$NO_3^- + H^+ \rightarrow HNO_3$	R11	$(H^+ + e^-) + NOH^* \rightarrow HNOH^*$
R1	$NO_3^- + H^+ + * \rightarrow HNO_3^*$	R12	$(H^+ + e^-) + HNO^* \rightarrow HNOH^*$
R2	$(H^+ + e^-) + HNO_3 + * \rightarrow NO_2^* + H_2O$	R13	$(H^+ + e^-) + HNO^* \rightarrow H_2NO^*$
R3	$(H^+ + e^-) + HNO_3^* \rightarrow NO_2^* + H_2O$	R14	$(H^+ + e^-) + H_2NO^* \rightarrow NH_2OH^*$
R4	$(H^+ + e^-) + NO_2^* \rightarrow cisHNO_2^*$	R15	$(H^+ + e^-) + HNOH^* \rightarrow NH_2OH^*$
R5	$(H^+ + e^-) + cisHNO_2^* \rightarrow NO^* + H_2O$	R16	$(H^+ + e^-) + NOH^* \rightarrow N^* + H_2O$
R6	$(H^+ + e^-) + NO_2^* \rightarrow HNO_2^*$	R17	$(H^+ + e^-) + HNOH^* \rightarrow NH^* + H_2O$
R7	$(H^+ + e^-) + NO_2^* \rightarrow HNO_2 + *$	R18	$(H^+ + e^-) + NH_2OH^* \rightarrow NH_2^* + H_2O$
R8	$HNO_2^* \rightarrow HNO_2 + *$	R19	$(H^+ + e^-) + N^* \rightarrow NH^*$
R9	$(H^+ + e^-) + NO^* \rightarrow NOH^*$	R20	$(H^+ + e^-) + NH^* \rightarrow NH_2^*$
R10	$(H^+ + e^-) + NO^* \rightarrow HNO^*$	R21	$(H^+ + e^-) + NH_2^* \rightarrow NH_3 + *$

Table S2. Adsorption energies (in eV) of intermediates involved in eNO_3RR on six MN_4 SACs.

Species \ Catalysts	CuN_4	NiN_4	CoN_4	FeN_4	VN_4	ScN_4
NO_2*	4.19	4.25	3.27	3.28	1.83	1.37
NO*	3.21	3.13	1.89	1.63	0.59	1.19
HNO_2*	3.63	3.60	3.44	3.27	2.26	2.47
$cisHNO_2$*	3.67	3.66	3.49	3.05	2.21	2.72
HNO_3*	5.24	5.27	5.27	5.23	2.97	3.87
HNO*	3.29	3.60	2.38	1.70	0.20	1.02
NOH*	4.30	4.28	3.10	2.28	0.58	2.50
HNOH*	2.98	3.04	2.05	1.81	0.60	0.84
H_2NO*	2.62	2.63	2.04	2.05	-0.31	-0.06
NH_2OH*	1.67	1.73	1.42	1.32	0.79	1.53
N*	4.45	4.60	3.10	2.01	-0.25	2.63
NH*	3.04	3.49	1.89	1.39	-1.45	1.09
NH_2*	1.10	1.33	0.17	-0.09	-1.64	-1.35
NO_3*	5.69	5.92	5.26	5.11	3.01	2.43

Table S3. The optimized adsorption structures of intermediates for eNO_3RR on six MN_4 SACs.

Species \ Catalysts	CuN_4	NiN_4	CoN_4	FeN_4	VN_4	ScN_4
NO_2*	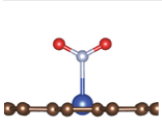	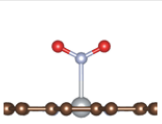	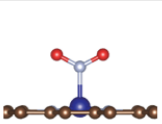	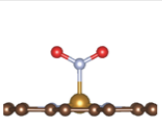	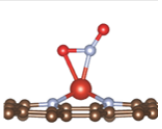	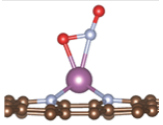
NO*	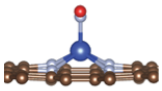	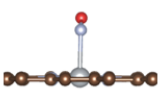	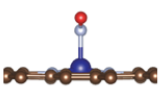	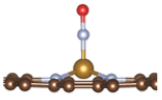	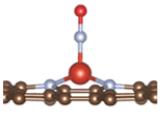	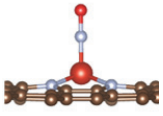
HNO_2*	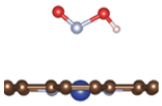	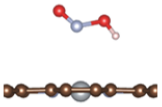	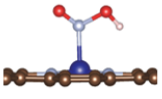	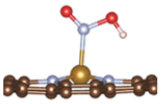	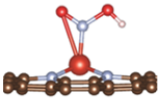	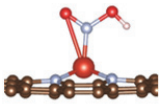
cisHNO_2*	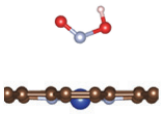	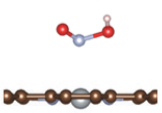	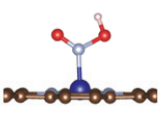	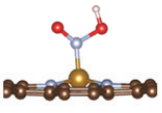	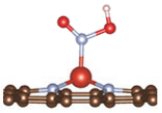	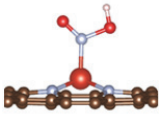
HNO_3*	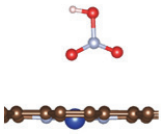	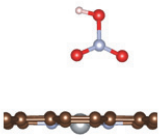	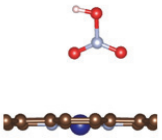	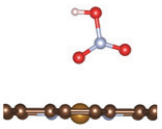	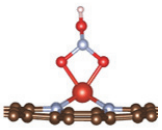	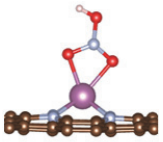
HNO*	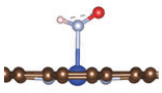	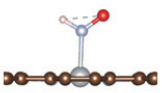	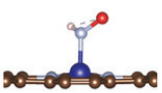	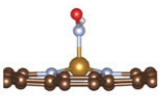	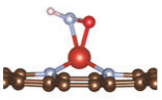	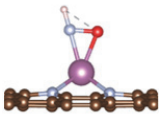
NOH*	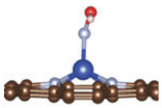	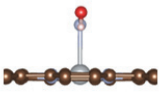	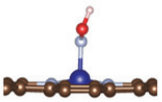	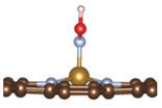		
HNOH*						
H_2NO*						

NH_2OH*	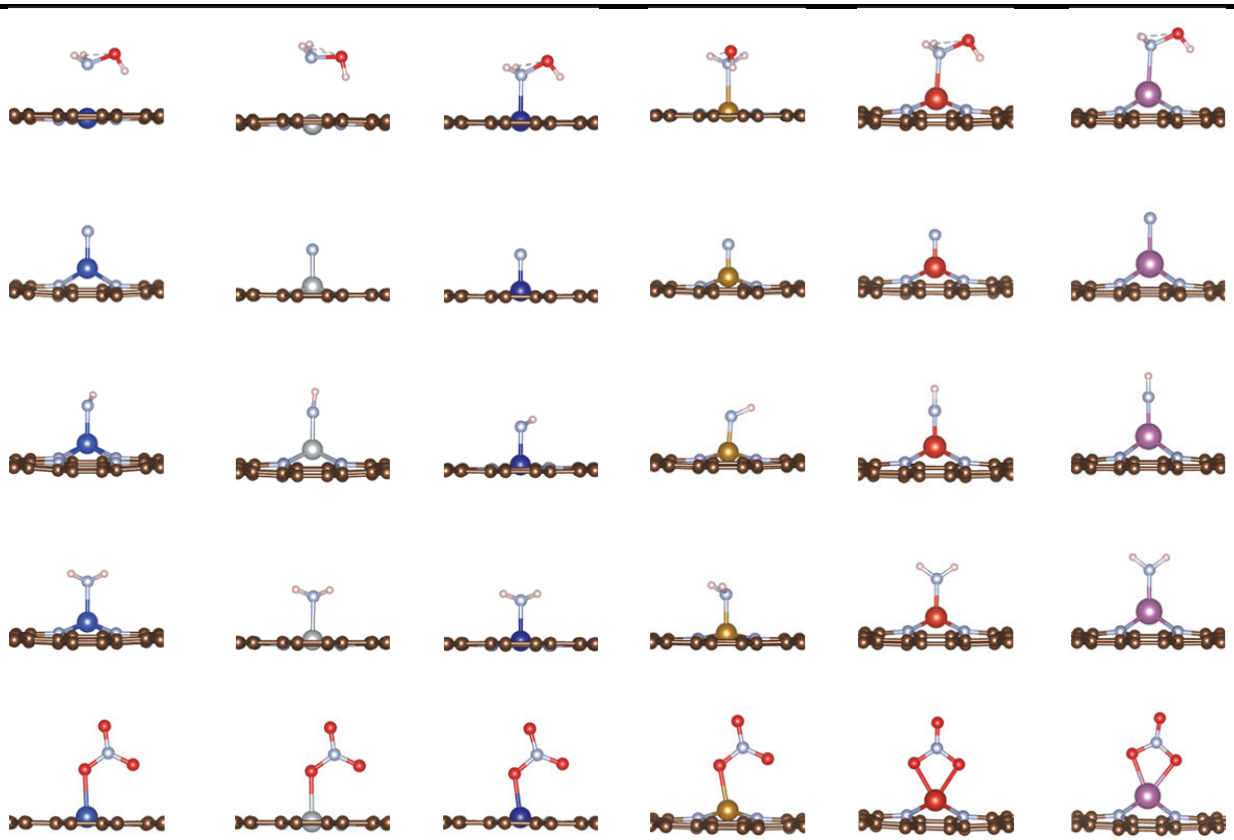
N*	
NH*	
NH_2*	
NO_3*	

Table S4. ΔE_{ZPE}-TΔS for intermediate species at 298.15 K.

Species	ZPE-TS (eV)	Species	ZPE-TS (eV)
HNO*	0.34	HNO_3*	0.34
NOH*	0.32	HNO_2*	0.33
HNOH*	0.60	$cisHNO_2$*	0.39
H_2NO*	0.61	N*	0.02
NH_2OH*	0.97	NH*	0.24
NO_2*	0.05	NH_2*	0.56
NO*	0.03	NO_3*	0.17

Table S5. Solvation energy corrections for adsorption energies of intermediate species.

Species	Solvation Energy (eV)	Species	Solvation Energy (eV)
HNO*	-0.18	HNO_3*	0.21
NOH*	-0.19	HNO_2*	-0.11
HNOH*	-0.20	cisHNO_2*	-0.16
H_2NO*	-0.38	N*	-0.07
NH_2OH*	-0.16	NH*	-0.16
NO_2*	-0.25	NH_2*	-0.10
NO*	0.00	NO_3*	-0.80

Table S6. The corrections of zero-point energy and entropy (in eV) for gas phase molecules at 298.15 K.

Species	ZPE[a]	TS[b]	ZPE-TS
H_2	0.27	0.40	-0.14
H_2O	0.54	0.58	-0.05
N_2	0.14	0.59	-0.45
NH_3	0.89	0.60	0.29
HNO_2	0.50	0.77	-0.27
HNO_3	0.65	0.83	-0.18

[a]Zero-point energies and [b]Entropies were taken from NIST Computational Chemistry Comparison and Benchmark Database. NIST Standard Reference Database Number 101 Release 22, May 2022, Editor: Russell D. Johnson III http://cccbdb.nist.gov/ DOI:10.18434/T47C7Z

Table S7. The summary of considered pathways for eNO_3RR to NH_3 and HNO_2 production.

NH_3 production	
Pathway (0): (0) $NO_3^- + H^+ \rightarrow HNO_3$ (2) $HNO_3 + (H^+ + e^-) + * \rightarrow NO_2* + H_2O$ (4) $NO_2* + (H^+ + e^-) \rightarrow cisHNO_2*$ (5) $cisHNO_2* + (H^+ + e^-) \rightarrow NO* + H_2O$ (10) $NO* + (H^+ + e^-) \rightarrow HNO*$ (13) $HNO* + (H^+ + e^-) \rightarrow H_2NO*$ (14) $H_2NO* + (H^+ + e^-) \rightarrow NH_2OH*$ (18) $NH_2OH* + (H^+ + e^-) \rightarrow NH_2* + H_2O$ (21) $NH_2* + (H^+ + e^-) \rightarrow NH_3 + *$	Pathway (1): (0) $NO_3^- + H^+ \rightarrow HNO_3$ (2) $HNO_3 + (H^+ + e^-) + * \rightarrow NO_2* + H_2O$ (4) $NO_2* + (H^+ + e^-) \rightarrow cisHNO_2*$ (5) $cisHNO_2* + (H^+ + e^-) \rightarrow NO* + H_2O$ (9) $NO* + (H^+ + e^-) \rightarrow NOH*$ (16) $NOH* + (H^+ + e^-) \rightarrow N* + H_2O$ (19) $N* + (H^+ + e^-) \rightarrow NH*$ (20) $NH* + (H^+ + e^-) \rightarrow NH_2*$ (21) $NH_2* + (H^+ + e^-) \rightarrow NH_3 + *$
Pathway (2): (1) $NO_3^- + H^+ + * \rightarrow HNO_3*$ (3) $HNO_3* + (H^+ + e^-) \rightarrow NO_2* + H_2O$ (4) $NO_2* + (H^+ + e^-) \rightarrow cisHNO_2*$ (5) $cisHNO_2* + (H^+ + e^-) \rightarrow NO* + H_2O$ (10) $NO* + (H^+ + e^-) \rightarrow HNO*$ (13) $HNO* + (H^+ + e^-) \rightarrow H_2NO*$ (14) $H_2NO* + (H^+ + e^-) \rightarrow NH_2OH*$ (18) $NH_2OH* + (H^+ + e^-) \rightarrow NH_2* + H_2O$ (21) $NH_2* + (H^+ + e^-) \rightarrow NH_3 + *$	Pathway (3): (1) $NO_3^- + H^+ + * \rightarrow HNO_3*$ (3) $HNO_3* + (H^+ + e^-) \rightarrow NO_2* + H_2O$ (4) $NO_2* + (H^+ + e^-) \rightarrow cisHNO_2*$ (5) $cisHNO_2* + (H^+ + e^-) \rightarrow NO* + H_2O$ (9) $NO* + (H^+ + e^-) \rightarrow NOH*$ (16) $NOH* + (H^+ + e^-) \rightarrow N* + H_2O$ (19) $N* + (H^+ + e^-) \rightarrow NH*$ (20) $NH* + (H^+ + e^-) \rightarrow NH_2*$ (21) $NH_2* + (H^+ + e^-) \rightarrow NH_3 + *$
Pathway (4): (0) $NO_3^- + H^+ \rightarrow HNO_3$ (2) $HNO_3 + (H^+ + e^-) + * \rightarrow NO_2* + H_2O$ (4) $NO_2* + (H^+ + e^-) \rightarrow cisHNO_2*$ (5) $cisHNO_2* + (H^+ + e^-) \rightarrow NO* + H_2O$ (9) $NO* + (H^+ + e^-) \rightarrow NOH*$ (11) $NOH* + (H^+ + e^-) \rightarrow HNOH*$ (15) $HNOH* + (H^+ + e^-) \rightarrow NH_2OH*$ (18) $NH_2OH* + (H^+ + e^-) \rightarrow NH_2* + H_2O$ (21) $NH_2* + (H^+ + e^-) \rightarrow NH_3 + *$	Pathway (5): (0) $NO_3^- + H^+ \rightarrow HNO_3$ (2) $HNO_3 + (H^+ + e^-) + * \rightarrow NO_2* + H_2O$ (4) $NO_2* + (H^+ + e^-) \rightarrow cisHNO_2*$ (5) $cisHNO_2* + (H^+ + e^-) \rightarrow NO* + H_2O$ (9) $NO* + (H^+ + e^-) \rightarrow NOH*$ (11) $NOH* + (H^+ + e^-) \rightarrow HNOH*$ (17) $HNOH* + (H^+ + e^-) \rightarrow NH* + H_2O$ (20) $NH* + (H^+ + e^-) \rightarrow NH_2*$ (21) $NH_2* + (H^+ + e^-) \rightarrow NH_3 + *$
Pathway (6): (0) $NO_3^- + H^+ \rightarrow HNO_3$ (2) $HNO_3 + (H^+ + e^-) + * \rightarrow NO_2* + H_2O$ (4) $NO_2* + (H^+ + e^-) \rightarrow cisHNO_2*$ (5) $cisHNO_2* + (H^+ + e^-) \rightarrow NO* + H_2O$ (10) $NO* + (H^+ + e^-) \rightarrow HNO*$ (12) $HNO* + (H^+ + e^-) \rightarrow HNOH*$ (15) $HNOH* + (H^+ + e^-) \rightarrow NH_2OH*$ (18) $NH_2OH* + (H^+ + e^-) \rightarrow NH_2* + H_2O$ (21) $NH_2* + (H^+ + e^-) \rightarrow NH_3 + *$	Pathway (7): (0) $NO_3^- + H^+ \rightarrow HNO_3$ (2) $HNO_3 + (H^+ + e^-) + * \rightarrow NO_2* + H_2O$ (4) $NO_2* + (H^+ + e^-) \rightarrow cisHNO_2*$ (5) $cisHNO_2* + (H^+ + e^-) \rightarrow NO* + H_2O$ (10) $NO* + (H^+ + e^-) \rightarrow HNO*$ (12) $HNO* + (H^+ + e^-) \rightarrow HNOH*$ (17) $HNOH* + (H^+ + e^-) \rightarrow NH* + H_2O$ (20) $NH* + (H^+ + e^-) \rightarrow NH_2*$ (21) $NH_2* + (H^+ + e^-) \rightarrow NH_3 + *$
Pathway (8): (1) $NO_3^- + H^+ + * \rightarrow HNO_3*$ (3) $HNO_3* + (H^+ + e^-) \rightarrow NO_2* + H_2O$ (4) $NO_2* + (H^+ + e^-) \rightarrow cisHNO_2*$ (5) $cisHNO_2* + (H^+ + e^-) \rightarrow H_2O + NO*$ (9) $NO* + (H^+ + e^-) \rightarrow NOH*$ (11) $NOH* + (H^+ + e^-) \rightarrow HNOH*$ (15) $HNOH* + (H^+ + e^-) \rightarrow NH_2OH*$ (18) $NH_2OH* + (H^+ + e^-) \rightarrow NH_2* + H_2O$ (21) $NH_2* + (H^+ + e^-) \rightarrow NH_3 + *$	Pathway (9): (1) $NO_3^- + H^+ + * \rightarrow HNO_3*$ (3) $HNO_3* + (H^+ + e^-) \rightarrow NO_2* + H_2O$ (4) $NO_2* + (H^+ + e^-) \rightarrow cisHNO_2*$ (5) $cisHNO_2* + (H^+ + e^-) \rightarrow H_2O + NO*$ (9) $NO* + (H^+ + e^-) \rightarrow NOH*$ (11) $NOH* + (H^+ + e^-) \rightarrow HNOH*$ (17) $HNOH* + (H^+ + e^-) \rightarrow NH* + H_2O$ (20) $NH* + (H^+ + e^-) \rightarrow NH_2*$ (21) $NH_2* + (H^+ + e^-) \rightarrow NH_3 + *$
Pathway (10): (1) $NO_3^- + H^+ + * \rightarrow HNO_3*$	Pathway (11): (1) $NO_3^- + H^+ + * \rightarrow HNO_3*$

(3) HNO_3* + (H^+ + e^-) → NO_2* + H_2O	(3) HNO_3* + (H^+ + e^-) → NO_2* + H_2O
(4) NO_2* + (H^+ + e^-) → cisHNO_2*	(4) NO_2* + (H^+ + e^-) → cisHNO_2*
(5) cisHNO_2* + (H^+ + e^-) → H_2O + NO*	(5) cisHNO_2* + (H^+ + e^-) → H_2O + NO*
(10) NO* + (H^+ + e^-) → HNO*	(10) NO* + (H^+ + e^-) → HNO*
(12) HNO* + (H^+ + e^-) → HNOH*	(12) HNO* + (H^+ + e^-) → HNOH*
(15) HNOH* + (H^+ + e^-) → NH_2OH*	(17) HNOH* + (H^+ + e^-) → NH* + H_2O
(18) NH_2OH* + (H^+ + e^-) → NH_2* + H_2O	(20) NH* + (H^+ + e^-) → NH_2*
(21) NH_2* + (H^+ + e^-) → NH_3 + *	(21) NH_2* + (H^+ + e^-) → NH_3 + *
HNO_2 production	
Pathway (12):	Pathway (13):
(0) NO_3^- + H^+ → HNO_3	(0) NO_3^- + H^+ → HNO_3
(2) HNO_3 + (H^+ + e^-) + * → NO_2* + H_2O	(2) HNO_3 + (H^+ + e^-) + * → NO_2* + H_2O
(6) NO_2* + (H^+ + e^-) → HNO_2*	(7) NO_2* + (H^+ + e^-) →HNO_2 + *
(8) HNO_2* → HNO_2 + *	
Pathway (14):	Pathway (15):
(1) NO_3^- + H^+ + * → HNO_3*	(1) NO_3^- + H^+ + * → HNO_3*
(3) HNO_3* + (H^+ + e^-) → NO_2* + H_2O	(3) HNO_3* + (H^+ + e^-) → NO_2* + H_2O
(6) NO_2* + (H^+ + e^-) → HNO_2*	(7) NO_2* + (H^+ + e^-) →HNO_2 + *
(8) HNO_2* → HNO_2 + *	

Table S8. Reaction free energies and activation barriers (in eV) of elementary reactions on FeN_4 for eNO_3RR in the optimal pathways at various potentials in microkinetic modeling.

Number	Elementary reactions	-0.50 V vs. RHE		-0.59 V vs. RHE		-0.66 V vs. RHE	
		ΔG	G_a	ΔG	G_a	ΔG	G_a
R0	$NO_3^- + H^+ \rightarrow HNO_3$	0.39	0.39	0.39	0.39	0.39	0.39
R2	$(H^+ + e^-) + HNO_3 + * \rightarrow NO_2* + H_2O$	-2.67	0.00	-2.76	0.00	-2.83	0.00
R4	$(H^+ + e^-) + NO_2* \rightarrow cisHNO_2*$	-0.30	0.55	-0.39	0.50	-0.46	0.46
R5	$(H^+ + e^-) + cisHNO_2* \rightarrow NO* + H_2O$	-2.11	0.39	-2.20	0.39	-2.27	0.39
R10	$(H^+ + e^-) + NO* \rightarrow HNO*$	-0.31	0.03	-0.40	0.00	-0.47	0.00
R12	$(H^+ + e^-) + HNO* \rightarrow HNOH*$	-0.15	0.00	-0.24	0.00	-0.31	0.00
R15	$(H^+ + e^-) + HNOH* \rightarrow NH_2OH*$	-0.59	0.00	-0.68	0.00	-0.75	0.00
R18	$(H^+ + e^-) + NH_2OH* \rightarrow NH_2* + H_2O$	-2.25	0.00	-2.34	0.00	-2.41	0.00
R21	$(H^+ + e^-) + NH_2* \rightarrow NH_3 + *$	-1.03	0.36	-1.12	0.36	-1.19	0.36
R7	$(H^+ + e^-) + NO_2* \rightarrow HNO_2 + *$	-0.01	0.48	-0.10	0.48	-0.17	0.48
Number	Elementary reactions	-0.73 V vs. RHE		-0.78 V vs. RHE		-0.85 V vs. RHE	
		ΔG	G_a	ΔG	G_a	ΔG	G_a
R0	$NO_3^- + H^+ \rightarrow HNO_3$	0.39	0.39	0.39	0.39	0.39	0.39
R2	$(H^+ + e^-) + HNO_3 + * \rightarrow NO_2* + H_2O$	-2.90	0.00	-2.95	0.00	-3.02	0.00
R4	$(H^+ + e^-) + NO_2* \rightarrow cisHNO_2*$	-0.53	0.42	-0.58	0.40	-0.65	0.36
R5	$(H^+ + e^-) + cisHNO_2* \rightarrow NO* + H_2O$	-2.34	0.39	-2.39	0.39	-2.46	0.39
R10	$(H^+ + e^-) + NO* \rightarrow HNO*$	-0.54	0.00	-0.59	0.00	-0.66	0.00
R12	$(H^+ + e^-) + HNO* \rightarrow HNOH*$	-0.38	0.00	-0.43	0.00	-0.50	0.00
R15	$(H^+ + e^-) + HNOH* \rightarrow NH_2OH*$	-0.82	0.00	-0.87	0.00	-0.94	0.00
R18	$(H^+ + e^-) + NH_2OH* \rightarrow NH_2* + H_2O$	-2.48	0.00	-2.53	0.00	-2.60	0.00
R21	$(H^+ + e^-) + NH_2* \rightarrow NH_3 + *$	-1.26	0.35	-1.31	0.35	-1.38	0.35
R7	$(H^+ + e^-) + NO_2* \rightarrow HNO_2 + *$	-0.24	0.47	-0.29	0.47	-0.36	0.47

Table S9. The geometries of IS, TS and FS of elementary steps for eNO_3RR on FeN_4.

Elementary steps	Geometries	Elementary steps	Geometries
$HNO_3+*\rightarrow NO_2*+H_2O$	IS 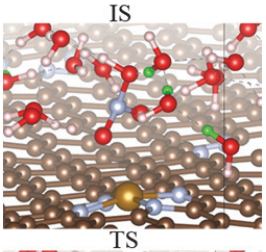 TS 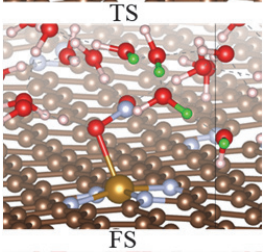 FS 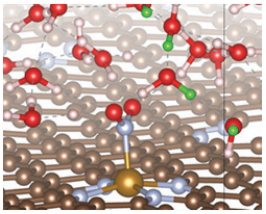	$NO_2*\rightarrow cisHNO_2*$	IS 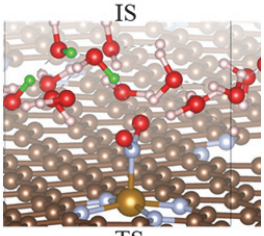 TS 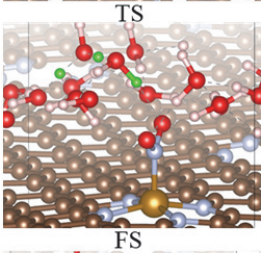 FS 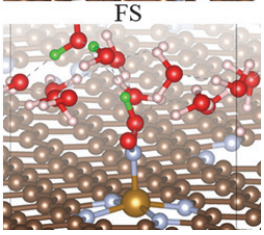
$cisHNO_2*\rightarrow NO*+H_2O$	IS 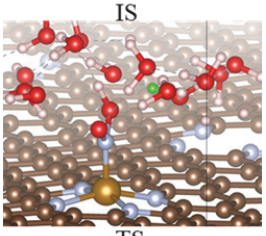 TS 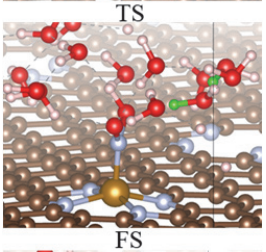 FS 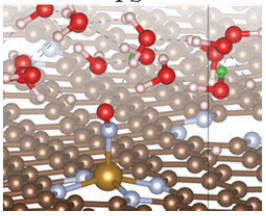	$NO*\rightarrow HNO*$	IS 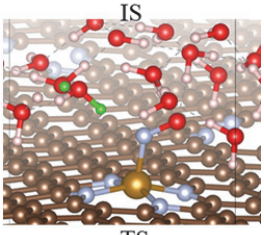 TS 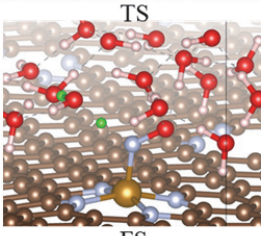 FS 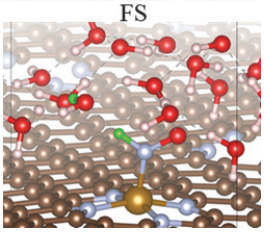

$HNO^*\rightarrow HNOH^*$	IS 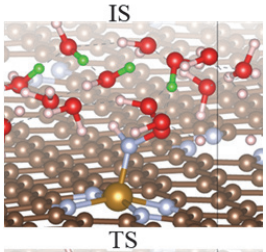 TS 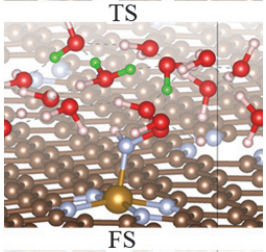 FS 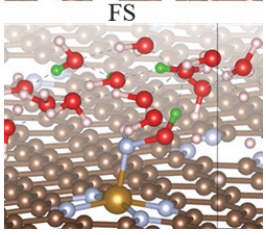	$HNOH^*\rightarrow NH_2OH^*$	IS 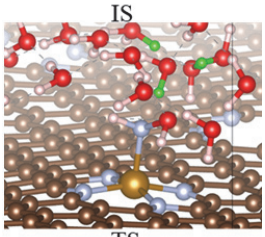 TS 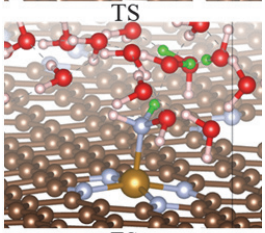 FS 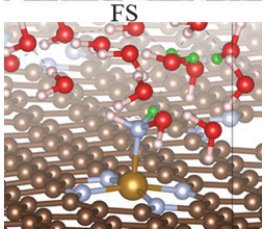
$NH_2OH^*\rightarrow NH_2^*+H_2O$	IS 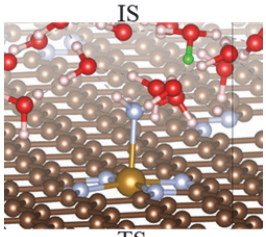 TS 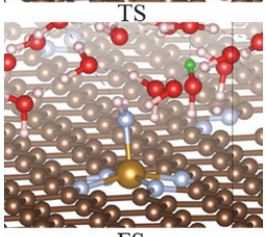 FS 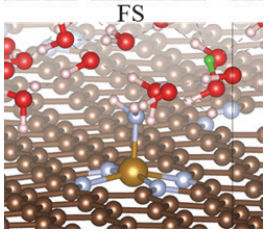	$NH_2^*\rightarrow NH_3$	IS 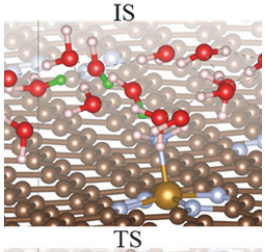 TS 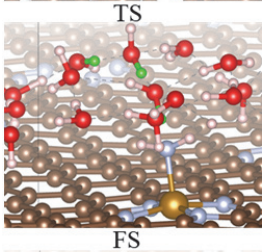 FS 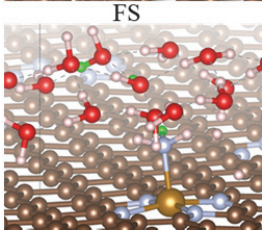

NO_2*→HNO_2*	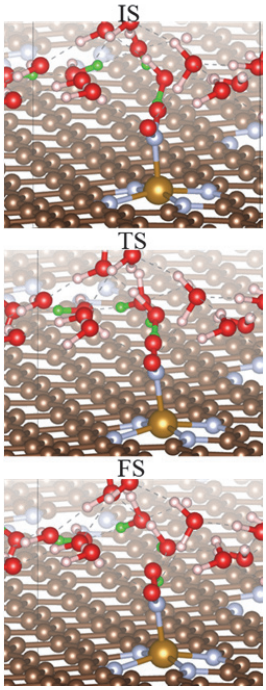	

Table S10. Kinetic equations of considered elementary steps in the microkinetic modeling for eNO_3RR to NH_3 and HNO_2.

Number	Elementary reactions	Reaction rate
R2	$(H^+ + e^-) + HNO_3 + * \rightarrow NO_2* + H_2O$	$r = k_f P_{HNO_3} P_{H^+} - k_b \theta_{NO_2^*} P_{H_2O}$
R4	$(H^+ + e^-) + NO_2* \rightarrow cisHNO_2*$	$r = k_f \theta_{NO_2^*} P_{H^+} - k_b \theta_{cisHNO_2^*}$
R5	$(H^+ + e^-) + cisHNO_2* \rightarrow NO* + H_2O$	$r = k_f \theta_{cisHNO_2^*} P_{H^+} - k_b \theta_{NO^*} P_{H_2O}$
R10	$(H^+ + e^-) + NO* \rightarrow HNO*$	$r = k_f \theta_{NO^*} P_{H^+} - k_b \theta_{HNO^*}$
R12	$(H^+ + e^-) + HNO* \rightarrow HNOH*$	$r = k_f \theta_{HNO^*} P_{H^+} - k_b \theta_{HNOH^*}$
R15	$(H^+ + e^-) + HNOH* \rightarrow NH_2OH*$	$r = k_f \theta_{HNOH^*} P_{H^+} - k_b \theta_{NH_2OH^*}$
R18	$(H^+ + e^-) + NH_2OH* \rightarrow NH_2* + H_2O$	$r = k_f \theta_{NH_2OH^*} P_{H^+} - k_b \theta_{NH_2^*} P_{H_2O}$
R21	$(H^+ + e^-) + NH_2* \rightarrow NH_3 + *$	$r = k_f \theta_{NH_2^*} P_{H^+} - k_b P_{NH_3}$
R7	$(H^+ + e^-) + NO_2* \rightarrow HNO_2 + *$	$r = k_f \theta_{NO_2^*} P_{H^+} - k_b P_{HNO_2}$

Table S11. The β of elementary steps on FeN_4 in the eNO_3RR to NH_3 and HNO_2 optimal pathways.

Number	Elementary reactions	β
R0	$NO_3^- + H^+ \rightarrow HNO_3$	-
R2	$(H^+ + e^-) + HNO_3 + * \rightarrow NO_2* + H_2O$	0.74
R4	$(H^+ + e^-) + NO_2* \rightarrow cisHNO_2*$	0.44
R5	$(H^+ + e^-) + cisHNO_2* \rightarrow NO* + H_2O$	0.01
R10	$(H^+ + e^-) + NO* \rightarrow HNO*$	0.41
R12	$(H^+ + e^-) + HNO* \rightarrow HNOH*$	0.04
R15	$(H^+ + e^-) + HNOH* \rightarrow NH_2OH*$	0.78
R18	$(H^+ + e^-) + NH_2OH* \rightarrow NH_2* + H_2O$	0.83
R21	$(H^+ + e^-) + NH_2* \rightarrow NH_3 + *$	0.03
R7	$(H^+ + e^-) + NO_2* \rightarrow HNO_2 + *$	0.03

Table S12. The FEs and NH_3 partial current in the eNO_3RR at various potentials on FeN_4 from Nat. Commun. 2021, 12 (1), 2870.

Potentials (V vs. RHE)	FE_{NH_3} (%)	FE_{HNO_2} (%)	NH_3 partial current (mA/cm^2)
-0.50	38.82	65.89	1.67
-0.59	65.20	28.67	9.30
-0.66	74.91	19.83	26.47
-0.73	70.71	14.44	50.90
-0.78	68.31	11.67	80.21
-0.85	66.77	9.15	98.61

References

[1] Mathew, K.; Kolluru, V. S. C.; Mula, S.; Steinmann, S. N.; Hennig, R. G., *J. Chem. Phys.* **2019,** *151* (23), 234101.

[2] Nørskov, J. K.; Rossmeisl, J.; Logadottir, A.; Lindqvist, L.; Kitchin, J. R.; Bligaard, T.; Jónsson, H., *J. Phys. Chem. B* **2004,** *108* (46), 17886-17892.

[3] Chan, K.; Norskov, J. K., *J Phys Chem Lett* **2015,** *6* (14), 2663-8.

[4] Chan, K.; Norskov, J. K., *J Phys Chem Lett* **2016,** *7* (9), 1686-90.

[5] Henkelman, G.; Uberuaga, B. P.; Jónsson, H., *J. Chem. Phys.* **2000,** *113* (22), 9901-9904.

[6] Liu, X.; Schlexer, P.; Xiao, J.; Ji, Y.; Wang, L.; Sandberg, R. B.; Tang, M.; Brown, K. S.; Peng, H.; Ringe, S.; Hahn, C.; Jaramillo, T. F.; Nørskov, J. K.; Chan, K., *Nat. Commun.* **2019,** *10* (1), 32.
[7] Long, J.; Guo, C.; Fu, X.; Jing, H.; Qin, G.; Li, H.; Xiao, J., *J. Phys. Chem. Lett.* **2021**, 6988-6995.
[8] Li, H.; Guo, C.; Fu, Q.; Xiao, J., *J Phys Chem Lett* **2019,** *10* (3), 533-539.
[9] Trasatti, S., *Pure Appl. Chem.* **1986,** *58* (7), 955-966.
[10] Wang, J. X.; Springer, T. E.; Adzic, R. R., *J. Electrochem. Soc.* **2006,** *153* (9), A1732.
[11] Lide, D. R.; Haynes, W. M., *CRC handbook of chemistry and physics*. CRC press Boca Raton, FL: 2010; Vol. 9.
[12] Wan, H.; Bagger, A.; Rossmeisl, J., *Angew. Chem. Int. Ed. Engl.* **2021,** *60* (40), 21966-21972.
[13] Chen, J.; Jia, M.; Hu, P.; Wang, H., *J. Comput. Chem.* **2021,** *42* (5), 379-391.
[14] Chen, J.-F.; Mao, Y.; Wang, H.-F.; Hu, P., *ACS Catal.* **2016,** *6* (10), 7078-7087.